Journal of Crystal Growth 485 (2018) 73–77

Contents lists available at ScienceDirect

Journal of Crystal Growth

journal homepage: www.elsevier.com/locate/crys

Single crystals with advanced laser properties $LiCaAlF_6:Ce^{3+}$ grown by Bridgman technique

A.A. Shavelev *, A.S. Nizamutdinov, M.A. Marisov, I.I. Farukhshin, O.A. Morozov, N.F. Rakhimov, E.V. Lukinova, S.L. Korableva, V.V. Semashko

Kazan Federal University, 420008, Kremlevskaja str., 18, Kazan, Russia

ARTICLE INFO

Article history:
Received 9 August 2017
Received in revised form 19 December 2017
Accepted 4 January 2018
Available online 5 January 2018
Communicated by R.S. Feigelson

Keywords:
A2. Single crystal growth
A2. Bridgman technique
B3. Solid state lasers
B3. Tunable ultraviolet laser

ABSTRACT

The aim of this work is growth of $LiCaAlF_6:Ce^{3+}$ (Ce:LiCAF) crystals by Bridgman technique and study of spectroscopic and laser characteristics in UV spectral range. We report on growth of $LiCaAlF_6:Ce^{3+}$ (1.2 at.% in the melt) crystals with refractive index inhomogeneity not worse than $\Delta n = 1.2 * 10^{-5}$. The maximum absorption coefficient of Ce^{3+} ions appeared to be up to 7 cm^{-1} and maximum of slope efficiency of laser action as high as 47% in synthesized crystals was achieved.

© 2018 Elsevier B.V. All rights reserved.

1. Introduction

$LiCaAlF_6:Ce^{3+}$ (Ce:LiCAF) crystal is a known and promising active medium for the ultraviolet spectral range [1–3]. The main advantage of the $LiCaAlF_6$ (LiCAF) host is the largest value of band gap (~100 000 cm^{-1}) among the known crystals [4] providing advantageous localization of energy states of impurities perspective for UV and VUV light amplification [5–7]. As a result, vibrationally broadened energy levels of Ce^{3+} ions fit within band-gap, minor influence of excited state absorption provides stable output laser characteristics, and active medium does not exhibit UV pump induced degradation [8–11], continuous wavelength tuning spreads over a relatively broad range 280–317 nm [12]. This lies in the course of industrial trends on shortening the wavelength of laser radiation and meets demand on robust and cheap in use laser sources.

Bridgman, Czochralski and micro-pulling down techniques are most popular among growth methods for obtaining of LiCAF crystals. But complexity of growing lies in the fact that components include aluminum fluoride which is volatile with a high value of saturated vapor pressure and which does not exist in a liquid state, so overheating of the melt leads to depletion of this component [13]. Also aluminum fluoride component exhibits significant water affinity which leads to a hydrolysis by residual water or hydroxyl groups in the crystal growth temperature range [13,14]. Growth procedure in the atmosphere of gaseous HF, CF_4, NH_4·HF or its mixtures with noble gases helps to maintain melt composition and to arrange fluorination [2,3,13,15–17]. Another peculiarity of Ce:LiCAF compound is extremely low segregation coefficient of trivalent rare earth ions due to heterogeneous substitution by factors of both valence and ionic radii [18]. Cations Ca^{2+} and Al^{3+} both have 6-fold coordination with fluorine anions in colquiriite crystal. The Ce^{3+} ion appears to substitute Ca^{2+} cation [19] where the ionic radius of Ce^{3+} is 1.15 Å which is close to that for Ca^{2+} (1.14 Å) while isovalent Al^{3+} is too small (0.67 Å) [20]. Heterovalent substitution necessitates charge compensation which causes lattice defects to appear when increasing the Ce^{3+} ions content. Usually investigators achieve absorption coefficient between 2 and 5 cm^{-1} in the maximum of absorption line (around 270 nm). It is important to achieve stable segregation of Ce^{3+} ions and to increase its value. This is inmortant in view of prospective of design distributed feedback lasers of UV spectral range and generation of picosecond pulses directly in UV [21–25].

The decision to use method of crystal growth by Bridgman was made due to the following reasons. The Bridgman technique allows growing crystals in closed graphite crucibles which serve for lower radiative coupling of melt, solid and furnace elements. This provides more stable melt/solid interface and lower loss in solid during cooling of the crystallized material [26]. Also positioning the melt above the crystal provides more stable axial distribution of temperature in contrast to Czochralski method when the hottest

* Corresponding author.
E-mail address: alexey.shavelev@gmail.com (A.A. Shavelev).

https://doi.org/10.1016/j.jcrysgro.2018.01.005
0022-0248/© 2018 Elsevier B.V. All rights reserved.

melt appears at the bottom of the ampoule thus providing significant convection determined distortions [27]. In the same work [26] it was also shown that convective flows occurring in the melt during Bridgman growth have far less influence on the process compared to Czochralski method thus providing faster growth process. This maintains the chemical composition of the melt and allows to produce crystal samples with various activator ions even if the segregation coefficients of the required impurities are extremely low, which is true for the investigated Ce:LiCAF crystals. Also colquiriite systems are multicomponent, and, as indicated above, it is crucial to arrange a sufficient temperature gradient in the crystallization zone during growth of these crystals [13].

Aim of this work is growth of $LiCaAlF_6$ crystals doped with Ce^{3+} ions in the amount of 1.2 at.% in the melt by Bridgman technique. Desired crystals are intended to be active media for UV lasers thus special attention has been payed to high optical quality of the synthesized material.

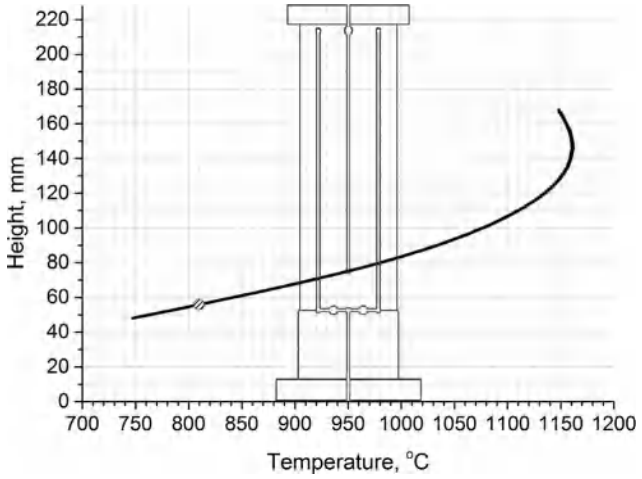

Fig. 1. Temperature dependence on height along the heater.

2. Preparation and growth by Bridgman technique

The crystal growth of LiCAF with Ce^{3+} ions content 1.2 at.% in the melt was performed using the Bridgman technique in the fluorinating atmosphere. The melting point is about 810 °C [17]. We used $Ar:CF_4$ gaseous mixture with the volume ratio 7:4 to fill the chamber after it's evacuation to 10^{-4} mbar. This ratio appeared to be optimal $Ar:CF_4$ from the point of view of quality of the crystallized material with respect to design of our heater and amount of charge material. The lower volumes of CF_4 lead to defects in crystals and higher volumes of CF_4 gave no better result. All initial components of the charge were preliminary treated to obtain purity not less than 99.99%. LiF, CaF_2 and CeF_3 components were taken from optical quality single crystals but CaF_2 and CeF_3 were regrown in high vacuum with addition of PbF_2. Besides, powder of CaF_2 for the charge was obtained by thermo-shock method [15]. AlF_3 was additionally fluorinated in order to remove traces of oxygen and hydroxyl groups in the crystals. To do that AlF_3 powder

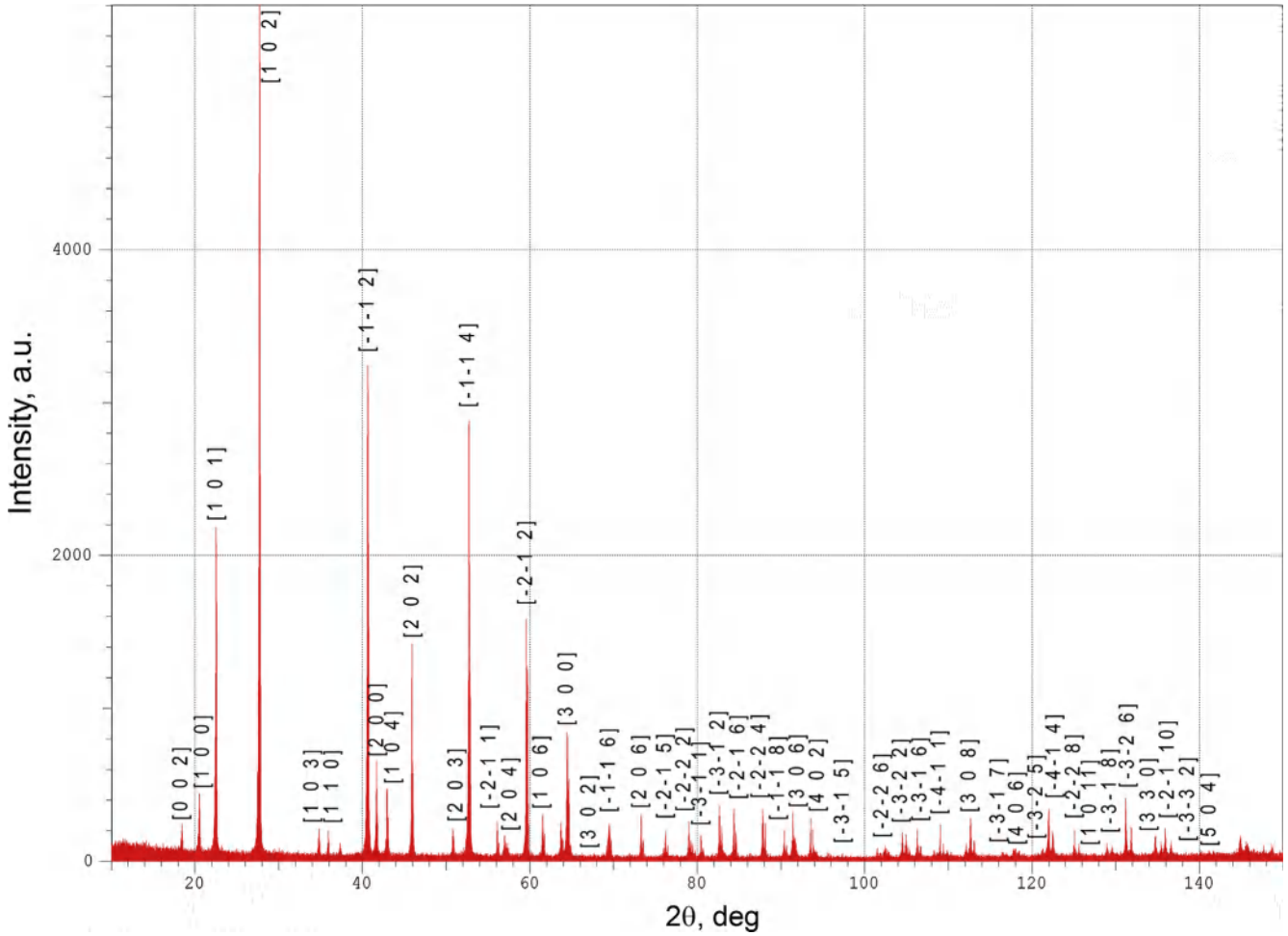

Fig. 2. X-ray diffraction pattern of the sample $LiCaAlF_6:Ce^{3+}$ with hkl indexes of planes for correspondent reflections.

with purity 99.99% was pumped to high vacuum (of about 10^{-4} mbar) in the growth chamber and was kept at temperature of about 800 °C [13] in CF_4 + Argon atmosphere (1:1). The resulting AlF_3 formed resembled transparent snowflakes with a size of 2–3 mm. Components of the charge of LiCAF to be grown were taken in ratios correspondent strongly to the stoichiometric composition.

Bridgman technique consists of pulling the crucible with overheated melt downwards through the heater from the high to the low temperature region. Heater assembly is of great importance since it determines other two demands for successful crystal growth: temperature stability and certain temperature gradient. We used axial resistive heater made of graphite and graphite crucible also. They were surrounded by heat shields with thermocouple mounted to stabilize the temperature with accuracy of about 0.1 °C. The wall thickness of the crucible was in the order of 1.5–2 mm to minimize distortion of the temperature field. Temperature distribution inside our heater measured along its axis is shown in Fig. 1. The measured temperature gradient was about 70 °C/cm.

The achieved temperature gradient was sufficient enough for the $LiCaAlF_6$ compound which melts congruently to crystallize with relatively high rates. Pulling rate of crucible in our experiments was 2 mm/hour. The LiCAF crystals were grown on seed crystals with the specified optical c-axis orientation perpendicular to the boule.

3. Characteristics of grown crystals

Obtained crystal boules were free of cracks and bubbles and had kept orientation of seeding crystal. Phase composition of crystallized material was investigated by means of X-ray diffractometry technique. The correspondent reflections distribution is shown at Fig. 2. The obtained diffraction pattern corresponds to colquiriite structure [28].

But obtained crystals exhibited volume scattering due to microscopic defects, the similar was described in work [29]. This was successfully removed by 48 h annealing at the temperature 10–15 °C below the melting point in CF_4 atmosphere [29,30]. In order to investigate optical quality and spectroscopic and laser properties a polished plane-parallel windows were made along the boules keeping plane of the windows parallel to the plane of optical c-axis. Length of the optical path in crystals Ce:LiCAF was 8 mm. The inhomogeneity of refractive index was controlled in Jamin interferometer and appeared to be not worse than $\Delta n = 1.2 * 10^{-5}$. The grown Ce:LiCAF crystal and its interference pattern are shown in Fig. 3.

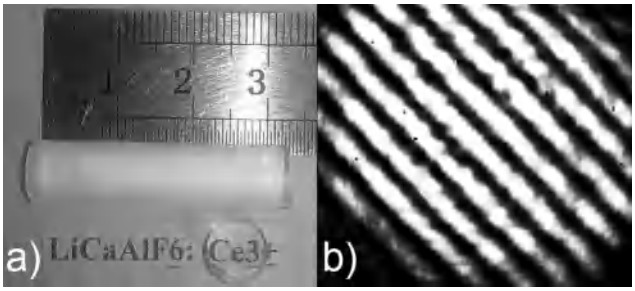

Fig. 3. The grown crystal $LiCaAlF_6:Ce^{3+}$ (a) and it's interference pattern from Jamin interferometer (b).

4. Spectroscopy and laser characteristics

Absorption and emission spectra of the grown Ce:LiCAF are shown in Fig. 4a. Absorption spectrum contains typical for Ce:LiCAF absorption band due to 4f-5d transitions which peaks at 270 nm with absorption coefficient about 7 cm^{-1}. The emission spectrum excited at 266 nm is also typical to Ce:LiCAF and has two peaks centered at 289 nm and 310 nm [1,12,16,17].

We have investigated the absorption coefficient along the boule of our Ce:LiCAF crystal. At Fig. 4b the integral under the 270 nm absorption band is presented as function of place at the crystal. The luminescence spectrum form as well as decay times has not changed along the crystal. The significant concentration gradient is clearly seen which is the evidence of low isomorphic capacity of LiCAF matrix in relation to Ce^{3+} ions. But there is an area of relatively plane characteristic in the middle of the boule with length of about 40 mm. The obtained dependence should allow to calculate the segregation coefficient of Ce^{3+} ions according to Gulliver-Pfann law, but in LiCAF crystal there are three types of Ce^{3+} impurity centers with absorption lines superposed give the observed absorption band.

The laser oscillation of the grown crystal was achieved under pulsed (10 ns pulse duration) laser pump at 266 nm in 10 cm long nonselective Fabry-Perot cavity with formed by two plane mirrors (99.9% and 60% reflectivity). The Ce:LiCAF crystal was turned to Brewster's angle with relation to cavity axis. Pump beam was longitudinally directed onto the crystal through refracting telescope

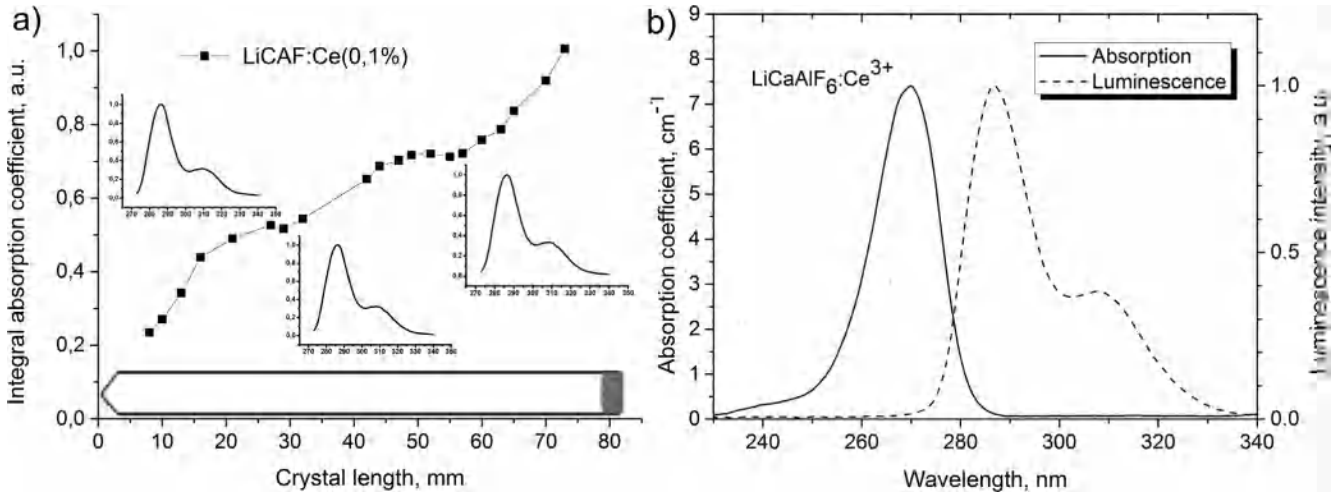

Fig. 4. (a) Integral under Ce^{3+} absorption band along the crystal, inlets show luminesce spectra at three points of the crystal; (b) Absorption and emission spectra of Ce:$LiCaAlF_6$.

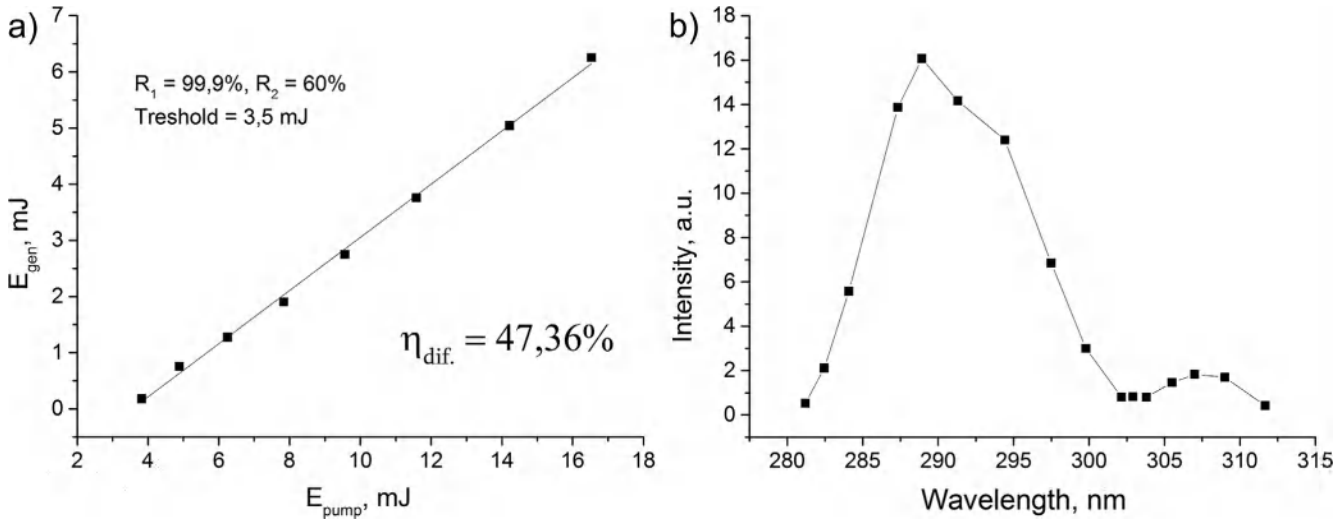

Fig. 5. (a) Dependence of laser energy on pump energy; (b) wavelength tuning curve of laser oscillation of Ce:$LiCaAlF_6$ active medium.

producing approximately 2 mm diameter waist. Both pump and lasing radiations corresponded to π polarization.

Pulsed laser oscillation of the Ce:LiCAF was obtained at 289 nm with 6 ns pulse duration. Lasing threshold was near 3 mJ and maximum of slope efficiency was up to 47% (Fig. 5a). This appears to be a high value since multicenter character of Ce^{3+} substitution in $LiCaAlF_6$ matrix when pump energy is being distributed among three types of centers and only one is lasing [18]. By simple inserting a 60° fused silica prism into a cavity we have achieved tuning from 281 nm to 312 nm. The intensity distribution is presented at Fig. 5b. This tuning range appears to be common.

5. Conclusion

$LiCaAlF_6:Ce^{3+}$ (1.2 at.% in the melt) crystal with high optical quality was obtained by Bridgman crystal growth technique and subsequent annealing. The refractive index inhomogeneity as it was measured in Jamin interferometer appeared to be no more than $\Delta n = 1.2 * 10^{-5}$. Absorption coefficient of 7 cm^{-1} for Ce^{3+} ions was achieved which has been relatively high and could speak for high rate of crystallization. Laser oscillation was obtained with the threshold near 3.5 mJ and slope efficiency up to 47% which is also high and speaks for high optical quality of the crystals.

Acknowledgements

Authors are grateful for financial support by the subsidy of the Russian Government (agreement No. 02.A03.21.0002) to support the Program of Competitive Growth of Kazan Federal University among World's Leading Academic Centers and for the subsidy allocated to Kazan Federal University for the state assignment in the sphere of scientific activities.

References

[1] M.A. Dubinskii et al., Ce^{3+}-doped colquiriite: a new concept of all-solid-state tunable ultraviolet laser, J. Mod. Opt. 40 (1993) 1–5.
[2] M.V. Luong et al., First-principles calculations of electronic and optical properties of $LiCaAlF_0$ and $LiSrAlF_6$ crystals as VUV to UV solid-state laser materials, Opt. Mater. 65 (2017) 15–20.
[3] Y. Yokota et al., Growth and scintillation properties of Ce: Li(Ca, Ba)AlF_6 scintillator crystals, IEEE Trans. Nucl. Sci. 61 (2014) 419–423.
[4] T. Shimizu et al., High pressure band gap modification of $LiCaAlF_6$, Appl. Phys. Lett. 110 (2017) 141902.
[5] E. Sarantopoulou et al., $LiCaAlF_6:Nd^{3+}$ crystal as optical material for 157 nm photolithography, Opt. Commun. 177 (2000) 377–382.
[6] Y. Minami et al., Temperature-dependent evaluation of Nd:LiCAF optical properties as potential vacuum ultraviolet laser material, Opt. Mater. 58 (2016) 5–8.
[7] V.V. Semashko et al., Problems in searching for new solid-state UV-and VUV-active media: the role of photodynamic processes, Phys. Solid State 47 (2005) 1507–1511.
[8] Y.Y. Kalisky, Solid State Lasers: Tunable Sources and Passive q-Switching Elements, SPIE Press, Bellingham, Washington, USA, 2014.
[9] T. Le et al., Low-threshold ultraviolet solid-state laser based on a Ce3+:$LiCaAlF_6$ crystal resonator, Opt. Lett. 37 (2012) 4961–4963.
[10] A.S. Nizamutdinov et al., Spectral kinetics of Ce^{3+} ions in double-fluoride crystals with a scheelite structure, Phys. Solid State 47 (2005) 1460–1462.
[11] A.S. Nizamutdinov et al., Optical and gain properties of series of crystals $LiF-YF_3-LuF_3$ doped with Ce^{3+} and Yb^{3+} ions, J. Lumin. 127 (2007) 71–75.
[12] V.A. Fromzel et al., Tunable, narrow linewidth, high repetition frequency Ce: LiCAF lasers pumped by the fourth harmonic of a diode-pumped Nd:YLF laser for ozone DIAL measurements, Adv. Opt. Photon. Dev., in: Ki Young Kim (Ed.), In Tech, 2010, pp. 101–116.
[13] D. Klimm et al., Melting behavior and growth of colquiriite laser crystals, Cryst. Res. Technol. 40 (2005) 352–358.
[14] D. Klimm et al., Ternary colquiriite type fluorides as laser hosts, Cryst. Res. Technol. 34 (1999) 145–152.
[15] J.T. Mouhovski, Control of oxygen contamination during the growth of optical calcium fluoride and calcium strontium fluoride crystals, Progress Cryst. Growth Character. Mater. 53 (2007) 79–116.
[16] A.A. Shavelev et al., Growth of solid solutions with colquiriite structure $LiCa_{0,2}Sr_{0,8}AlF_6:Ce^{3+}$, J. Phys.: Conference Series – IOP Publishing 560 (2014) (012001).
[17] V.K. Castillo et al., Material and laser characterization of Intermediate Compositions of Ce:LiSrCaA1F_6, Proc. SPIE. 3929 (2000) 129–132.
[18] V.V. Semashko et al., Investigation of multisite activation in $LiCaAlF_6:Ce^{3+}$ crystals using stimulated quenching of luminescence, Laser Phys. 5 (1995) 69–72.
[19] R.Yu. Abdulsabirov et al., Crystal growth, EPR and site-selective laser spectroscopy of Gd^{3+}-activated $LiCaALF_6$ single crystals, J. Lumin. 94 (2001) 113–117.
[20] R.D. Shannon et al., Revised effective ionic radii and systematic studies of interatomic distances in halides and chalcogenides, Acta Crystallogr. A 32 (1976) 751–767.
[21] T. Le, Schowalter, et al., Low-threshold ultraviolet solid-state laser based on a Ce^{3+}:$LiCaAlF_6$ crystal resonator, Opt. Lett. 37 (2012) 4961–4963.
[22] J.F. Pinto et al., Distributed-feedback, tunable Ce^{3+}-doped colquiriite lasers, Appl. Phys. Lett. 71 (1997) 205–207.
[23] M.H. Pham et al., Numerical simulation of ultraviolet picosecond Ce: LiCAF laser emission by optimized resonator transients, Jpn. J. Appl. Phys. 53 (2014) 062701.
[24] Z. Liu et al., Subnanosecond tunable ultraviolet pulse generation from a low-Q, short-cavity Ce:LiCAF laser, Jpn. J. Appl. Phys. Part 2: Lett. 36 (1997) 1384–1386.
[25] I.I. Farukhshin et al., Ultra-short pulses UV lasing in multifunctional Ce: $LiY_{0,3}Lu_{0,7}F_4$ active medium, Opt. Mater. Exp. 6 (2016) 1131–1137.
[26] S. Brandon et al., Heat transfer in vertical Bridgman growth of oxides: effects of conduction, convection, and internal radiation, J. Cryst. Growth 121 (1992) 473–494.

[27] C.J. Chang et al., Radial segregation induced by natural convection and melt/solid interface shape in vertical Bridgman growth, J. Cryst. Growth 63 (1983) 343–364.
[28] S. Kuze et al., Structures of $LiCaAlF_6$ and $LiSrAlF_6$ at 120 and 300 K by synchrotron X-ray single-crystal diffraction, J. Solid State Chem. 177 (2004) 3505–3513.
[29] J.J. De Yoreo et al., Elimination of scattering centers from Cr:$LiCaAlF_6$, J. Cryst. Growth 113 (1991) 691–697.
[30] D. Klimm et al., Morphologic defects in Cr3+: LiCaAlF6 crystals grown by the Czochralski method, in: XII Conference on Solid State Crystals: Materials Science and Applications. – International Society for Optics and Photonics, 1997, pp. 35–41.